ANALYTIC FORMULATION OF THE STOCHASTIC ENERGIZATION-RELAXATION CHANNEL MODEL OF PROTON PUMPING BY BACTERIAL RHODOPSINS

MONICA NEAGU

Center for Modeling Biological Systems and Data Analysis, Department of Functional Sciences, "Victor Babeş" University of Medicine and Pharmacy Timişoara, 2–4, Eftimie Murgu square, 300041 Timişoara, Romania, e-mail: maneagu@yahoo.com

Abstract. The active transport of ions builds and maintains electrochemical potential gradients across biological cell membranes. It is performed by ion pumps: membrane proteins fueled by energy-releasing processes. The stochastic energization-relaxation channel (SERC) model of active transport describes the pump as a multi-ion channel with two conformations, termed energized and relaxed, of specific free energy profiles. Here we present a new, analytic formulation of the SERC model, based on differentiation formulae from the theory of stochastic differential equations. The energization/relaxation switches are described in terms of a Markovian dichotomous noise. Upon averaging the kinetic equations over the noise, the mean ion flux per pump molecule is obtained as a function of time. Its asymptotic value, the stationary ion flux generated by one transport protein, is a measurable quantity, found to be in qualitative agreement with experimental results on bacteriorhodopsin, a light-driven proton pump.

Key words: Markovian dichotomous noise, Shapiro-Loginov theorem.

INTRODUCTION

Living cells hinge on the active transport of ions across cell and organelle membranes against thermodynamic forces. Active transport is carried out by proteins that couple an energy releasing process, such as adenosine triphosphate (ATP) hydrolysis or photon uptake, to the transmembrane movement of ions [14]. The mechanism of active transport, by which a scalar or locally vectorial process drives the directional movement of ions through the membrane protein (also called ion pump), is not fully understood [17]. It has long been argued that during pumping the transporter must assume at least two distinct conformational states [6], and Tanford proposed the today widely accepted alternative access model of

Received: December 2015;
in final form January 2016.

ROMANIAN J. BIOPHYS., Vol. 25, No. 4, P. 233–245, BUCHAREST, 2015

substrate translocation [22]. Läuger suggested a channel-like structure for the transport protein [13, 14]; subsequent experiments support his conjecture [5, 17].

In the stochastic energization-relaxation channel (SERC) model of vectorial ion transport [18, 19, 20], the transporter is viewed as a multi-ion channel [9] with two main conformations, referred to as energized and relaxed states. These are characterized by distinct free energy profiles. The assumption is that switches between them occur stochastically and are powered by an energy supplying process. Monte Carlo simulations revealed the qualitative agreement between model predictions and experiments [18, 19, 20].

MATERIALS AND METHODS

We consider a proton pump with three proton binding sites [19]. The simple kinetic model of single-ion occupancy is described by a cyclic, four-state reaction scheme (Fig. 1A), in which 1 stands for the empty configuration, in which no proton is bound to the active transport protein.

We assume that during transition $1\rightarrow 2$ a cytoplasmic proton is bound to the first binding site. Hence, the corresponding rate constant, k_{21}, is pseudomonomolecular; it contains the cytoplasmic concentration of the transported ion: $k_{21} = k_{21}^{*}[\mathrm{H}^{+}]_{\mathrm{int}}$, where k_{21}^{*} is a bimolecular rate constant. Similarly, the process $4\rightarrow 1$ leads to the release of a proton into the surrounding medium, and the rate constant of the inverse transition, $k_{41} = k_{41}^{*}[\mathrm{H}^{+}]_{\mathrm{ext}}$, incorporates the extracellular proton concentration. These rate constants account for the pH sensitivity of the model.

The rate constants for the transport of electrically charged particles depend on the transmembrane electric field according to the Boltzmann relation:

$$k_{ij} = k_{ij}^{0} \exp\left(\frac{zF\Delta\psi}{RT} \alpha_{ij} d_{ij} \right), \tag{1}$$

where we have denoted by $\Delta\psi \equiv \psi_{\mathrm{int}} - \psi_{\mathrm{ext}}$ the electric potential difference between the intra- and extracellular media, k_{ij}^{0} corresponds to $\Delta\psi = 0$, whereas $d_{ij} = d_{ji}$ are fractions of the membrane potential traversed by the transported ion, of valence z, during the $j \rightarrow i$ or $i \rightarrow j$ processes, respectively. These are dimensionless numbers between 0 and 1, also called electrical distances, and are not to be confused with physical ones.

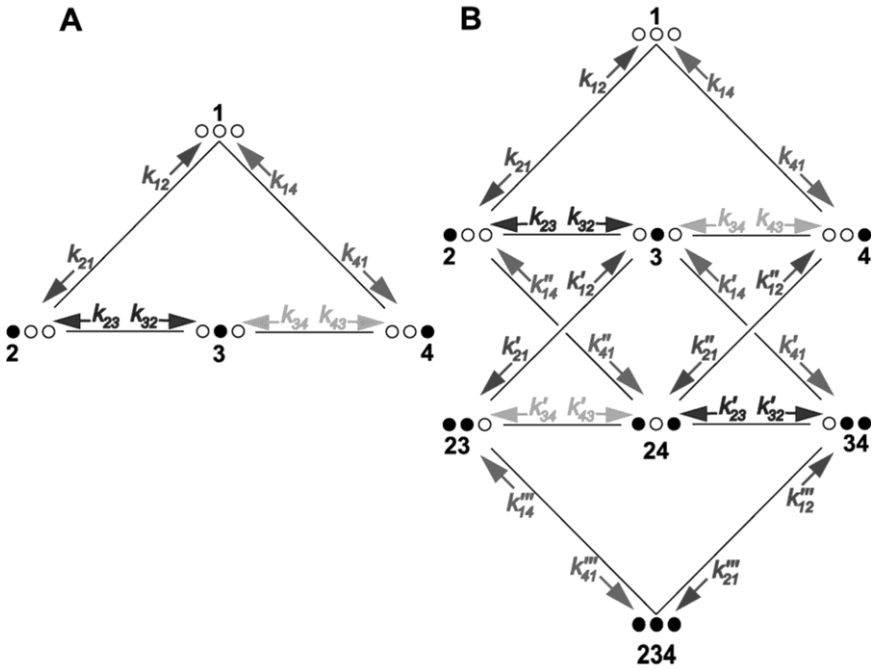

Fig. 1. Reaction cycle of a proton pump with three ion-binding sites at single (A) and multiple occupancy (B). Dark dots signify occupied sites. The left circle from each triplet represents the site closest to the cytoplasm, whereas the right one stands for the site facing the extracellular medium. Primed rate constants may differ from the unprimed ones due to electrostatic repulsion between ions in the pump or conformational changes induced by site occupation; here we take $k_{ij} = k'_{ij} = k''_{ij} = k'''_{ij}$.

The rate constants used in this work are: for the relaxed state $k_{21}^{*\,\mathrm{relaxed}} = 10^{11}\ \mathrm{M^{-1}s^{-1}}$, $k_{12}^{\mathrm{relaxed}} = 1\ \mathrm{s^{-1}}$, $k_{32}^{\mathrm{relaxed}} = 10^{2}\ \mathrm{s^{-1}}$, $k_{23}^{\mathrm{relaxed}} = 1\ \mathrm{s^{-1}}$, $k_{43}^{\mathrm{relaxed}} = 10^{-8}\ \mathrm{s^{-1}}$, $k_{34}^{\mathrm{relaxed}} = 10^{2}\ \mathrm{s^{-1}}$, $k_{14}^{\mathrm{relaxed}} = 10^{7}\ \mathrm{s^{-1}}$, $k_{41}^{*\,\mathrm{relaxed}} = 10^{10}\ \mathrm{M^{-1}s^{-1}}$ and for the energized state $k_{21}^{*\,\mathrm{energized}} = 10^{11}\ \mathrm{M^{-1}s^{-1}}$, $k_{12}^{\mathrm{energized}} = 1\ \mathrm{s^{-1}}$, $k_{32}^{\mathrm{energized}} = 10^{-6}\ \mathrm{s^{-1}}$, $k_{23}^{\mathrm{energized}} = 10^{3}\ \mathrm{s^{-1}}$, $k_{43}^{\mathrm{energized}} = 10^{3}\ \mathrm{s^{-1}}$, $k_{34}^{\mathrm{energized}} = 10^{2}\ \mathrm{s^{-1}}$, $k_{14}^{\mathrm{energized}} = 10^{7}\ \mathrm{s^{-1}}$, $k_{41}^{*\,\mathrm{energized}} = 10^{10}\ \mathrm{M^{-1}s^{-1}}$ [19].

The partitioning coefficients, α_{ij}, give the fraction of the potential drop, $d_{ij}(\psi_{\mathrm{ext}} - \psi_{\mathrm{int}})$, which has to be traversed during the $j \to i$ process in order to reach the maximum of the corresponding energy barrier. Their sign depends on the direction of charge translocation; in our context they are positive for rate constants of forward transitions. The requirement of equilibrium detailed balance [7, 14] is satisfied if $\alpha_{ij} - \alpha_{ji} = 1$. For symmetric barriers, with energy maxima lying halfway between neighboring minima [9], we have $\alpha_{ij} = -\alpha_{ji} = 1/2$. Throughout

the paper, T stands for the absolute temperature, whereas R and F denote the gas constant and Faraday's constant, respectively. We use the rate constants from the caption of Fig. 1, proposed for simulations of bacteriorhodopsin [19].

Suppose that we have N pumps in the membrane under study and that, at a given moment, N_i of these are in state i. The system may be described by the set of mole fractions, $p_i \equiv N_i / N$, which may be viewed as the probabilities of finding a pump in the states labeled by the index i. Since in the single-ion channel model each pump is supposed to be in either of the states 1, 2, 3 or 4, shown in Fig. 1A, the mole fractions satisfy the normalization relation $\sum_{i=1}^{4} p_i = 1$. In the absence of energization-relaxation jumps, the kinetic equations associated to the reaction cycle of Fig. 1A read:

$$\frac{\mathrm{d}p}{\mathrm{d}t} = Kp \tag{2}$$

where p stands for the column vector of components p_1, p_2, p_3, p_4, and

$$K = \begin{bmatrix} -k_{41} - k_{21} & k_{12} & 0 & k_{14} \\ k_{21} & -k_{12} - k_{32} & k_{23} & 0 \\ 0 & k_{32} & -k_{23} - k_{43} & k_{34} \\ k_{41} & 0 & k_{43} & -k_{34} - k_{14} \end{bmatrix} \tag{3}$$

The solution may be written as a linear combination, $p(t) = \sum_{i=1}^{4} A_i V_i \exp(v_i t)$, where v_i are the eigenvalues of K and V_i denotes the normalized eigenvector corresponding to the eigenvalue v_i. The integration constants, A_i, are determined by the initial condition. Being mainly interested in the stationary properties of the system, obtained asymptotically at $t \to \infty$, we may choose the initial condition arbitrarily. The ion flux per pump molecule is given by $\varphi = k_{14} p_4 - k_{41} p_1$.

Multi-ion models have been proposed earlier to explain the selectivity of ion channels [8, 9]. They also account for high throughput since site occupancy limits the set of possible transitions. Fig. 1B depicts the corresponding reaction scheme. The state of the system will be specified again by mole fractions, which satisfy the normalization condition $p_1 + p_2 + p_3 + p_4 + p_{23} + p_{24} + p_{34} + p_{234} = 1$. Here

indices refer to occupied sites except for the first term, which is the fraction of empty pumps. The kinetic equations may be solved, just as in the case of single-ion occupancy, by numerically solving the associated eigenvalue problem and using the analytic solution of the system. The numerical solutions of the eigenvalue problems were obtained using MATLAB (The MathWorks, Inc., Natick, MA, USA).

The ion flux per pump in this context may be written as: $\varphi = k_{14}\left(p_4 + p_{24} + p_{34} + p_{234}\right) - k_{41}\left(p_1 + p_2 + p_3 + p_{23}\right)$.

An energization or relaxation process, that is, a jump between the two free energy profiles [18], may be implemented using a symmetric Markovian dichotomous noise of unit norm, defined by the properties [4, 10]:

$$\xi(t) \in \{-1, 1\}, \tag{4a}$$

$$\left\langle \xi(t) \right\rangle = 0, \tag{4b}$$

$$\left\langle \xi(t)\xi(t') \right\rangle = \exp(-\lambda \mid t - t' \mid). \tag{4c}$$

This is a particular case of a dichotomic Markov process [23] with values $\Delta = +1$ and $\Delta' = -1$ of average duration τ_Δ and $\tau_{\Delta'}$, respectively. The requirement of vanishing time average, Eq. (4b), implies $\Delta\tau_\Delta + \Delta'\tau_{\Delta'} = 0$. Eq. (4c) gives the time autocorrelation function of the noise. The parameter λ is the inverse of the noise correlation time, τ_c; it is given by $\lambda \equiv 1/\tau_c = 1/\tau_\Delta + 1/\tau_{\Delta'}$. In the particular case of a symmetric noise of unit norm, the mean lifetimes of each value of the random variable are equal, $\tau_\Delta = \tau_{\Delta'} = 2\lambda^{-1}$. Thus, the average frequency of jumps undergone by $\xi(t)$ is $\lambda/2$ and, since every other jump is an energization, the average frequency of energizations is $\lambda/4$.

We write the kinetic equations of the system with energization/relaxation switches occurring at random instants of time, by replacing the rate constants with the stochastically fluctuating quantities

$$\tilde{k}_{ij} = k_{ij} \exp\left[-a_{ij}\,\xi(t)\right], \tag{5}$$

where $a_{ij} = \frac{1}{2}\ln\left[\frac{k_{ij}^{\text{relaxed}}}{k_{ij}^{\text{energized}}}\right]$ are dimensionless noise amplitudes responsible for the switch between the rate constants associated to the relaxed and energized state, and

$k_{ij} = \sqrt{k_{ij}^{\text{relaxed}} k_{ij}^{\text{energized}}}$. Averaging the kinetic equations over the realizations of the random variable $\xi(t)$, we obtain a system of differential equations for the noise-averaged mole fractions $\langle p_i \rangle$, but, along with these, new unknown functions arise, $\langle \xi\, p_i \rangle$; thus, the system needs to be completed to twice as many equations as in the fluctuation-free case. To this end, we use the Shapiro-Loginov theorem [3, 15, 21]:

$$\frac{\mathrm{d}}{\mathrm{d}t}\langle \xi\, p_i \rangle = -\lambda \langle \xi\, p_i \rangle + \left\langle \xi\, \frac{\mathrm{d}p_i}{\mathrm{d}t} \right\rangle, \tag{6}$$

and obtain the system of equations

$$\frac{\mathrm{d}x}{\mathrm{d}t} = Mx \tag{7}$$

for the unknown vector $x(t) = [\langle p_1 \rangle, \langle p_2 \rangle, \ldots, \langle \xi\, p_1 \rangle, \langle \xi\, p_2 \rangle, \ldots]^{\perp}$, where $\perp$ denotes matrix transposition. Straightforward calculations lead to the conclusion that, in both models, the matrix from Eq. (7) reads:

$$M = \begin{vmatrix} P & Q \\ Q & P - \lambda \mathrm{I} \end{vmatrix} \tag{8}$$

where I stands for the unit matrix of the size of the system matrix from the jump-free case (e.g. K of Eq. (3) in the single-ion model), whereas P and Q may be obtained from K by substituting k_{ij} with $k_{ij}\cosh(a_{ij})$ and $k_{ij}\sinh(a_{ij})$, respectively.

RESULTS

In the absence of energization/relaxation jumps, i.e. when the free energy profile of the pump remains unchanged, no stationary flux emerges (results not shown), as dictated by detailed balance for both the energized and relaxed state rate constants [7].

When switches between these states occur at random instants of time, described in our formalism by the noise-averaged kinetic equations (Eq. (7)), the stationary ion flux is noteworthy if the mean time between subsequent

energizations (the cycle duration), $\tau = 4\lambda^{-1}$, is short enough. This is exemplified in Fig. 2 by the time course of the pump flux in the presence of noise. The starting point of this evolution was specified by the initial condition imposed for Eq. (7): $\langle p_{23} \rangle = 1$ and all the other components of $x(0)$ were taken as zero to mimic the initial state of the bacteriorhodopsin photocycle [16]. Note that, for the rate constants given in the caption of Fig. 1, the asymptotic value of the flux becomes significant as τ drops below one second, increases with decreasing τ, and reaches saturation at cycle durations of about 10^{-4} s.

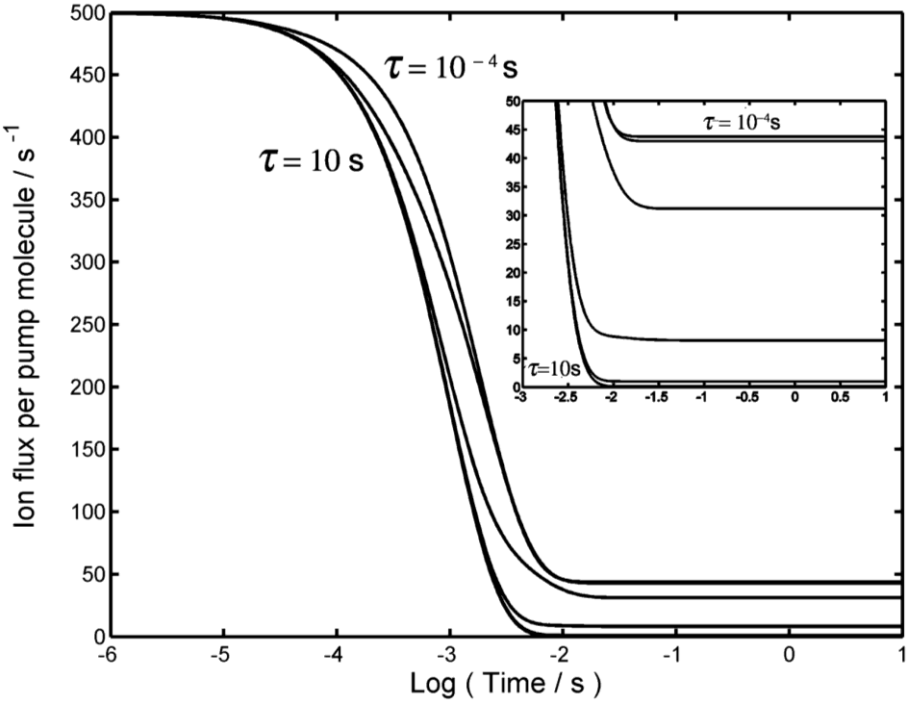

Fig. 2. The proton flux of a pump *vs.* the decimal logarithm of time, for 6 different energization-relaxation cycle durations given by integer powers of 10 ranging from 10^{-4} s to 10 s. The inset depicts details of the same plot for log (time/s) in the range (–3) to 1 and Ion flux per pump molecule between 0 and 50. See the caption of Fig. 1 for rate constants.

The impact of pH on proton pumping is illustrated in Fig. 3, where the membrane is supposed to be bathed on both sides by solutions of the same pH.

In the SERC model the coupling between energy input and ion translocation is stochastic and loose, characterized by the coupling efficiency, defined as the

average number of ions transported by one pump due to one energization [19]. In the present framework the coupling efficiency, η, is given by the noise-averaged pump flux multiplied by the cycle duration, *i.e.* $\eta = 4\lambda^{-1}\langle\varphi\rangle$.

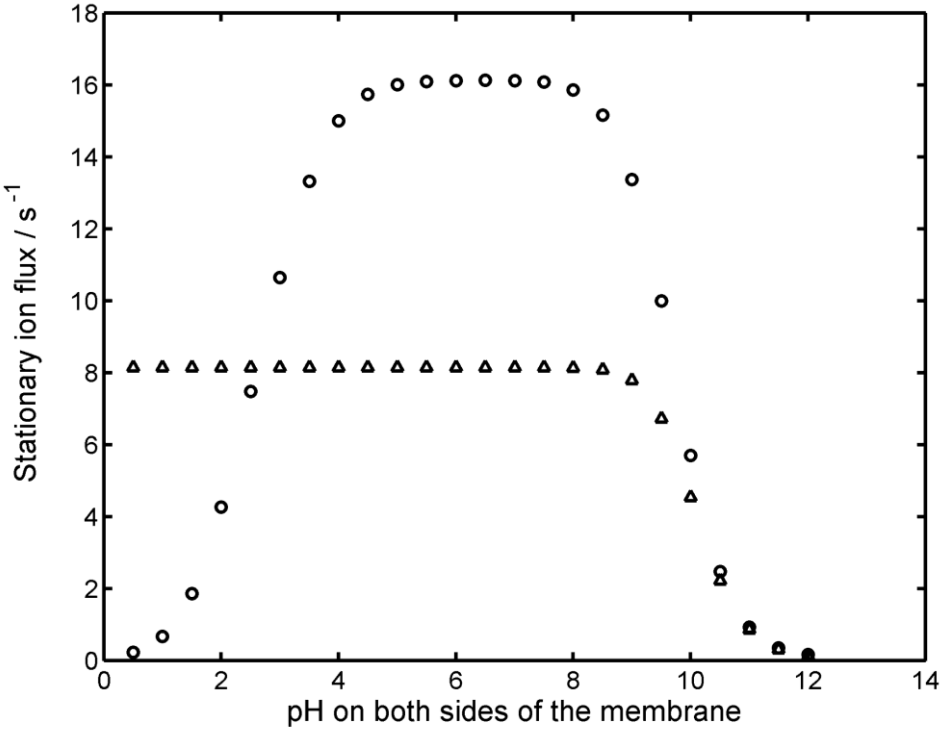

Fig. 3. The stationary ion flux per pump molecule *vs.* the pH of surrounding media. Triangular markers result from the single-ion model, whereas circles arise from the model with multiple occupancy of the active transporter. Here we set the cycle duration to 40 ms and used the rate constants given in the caption of Fig. 1.

By multiplying the stationary ion flux by η we obtain a convenient measure of the conditions under which both good coupling ratio and high flux are achieved.

Shown in Figs. 4 and 5 are the coupling efficiency and the product of the stationary flux and the coupling efficiency; Fig. 4 characterizes the single-ion model, whereas Fig. 5 characterizes the multi-ion model.

The surface plot of Fig. 4A shows the influence of membrane voltage and cycle duration on the coupling efficiency. Fig. 4B shows the impact of voltage and flipping-rate on the product of the stationary flux and the coupling efficiency.

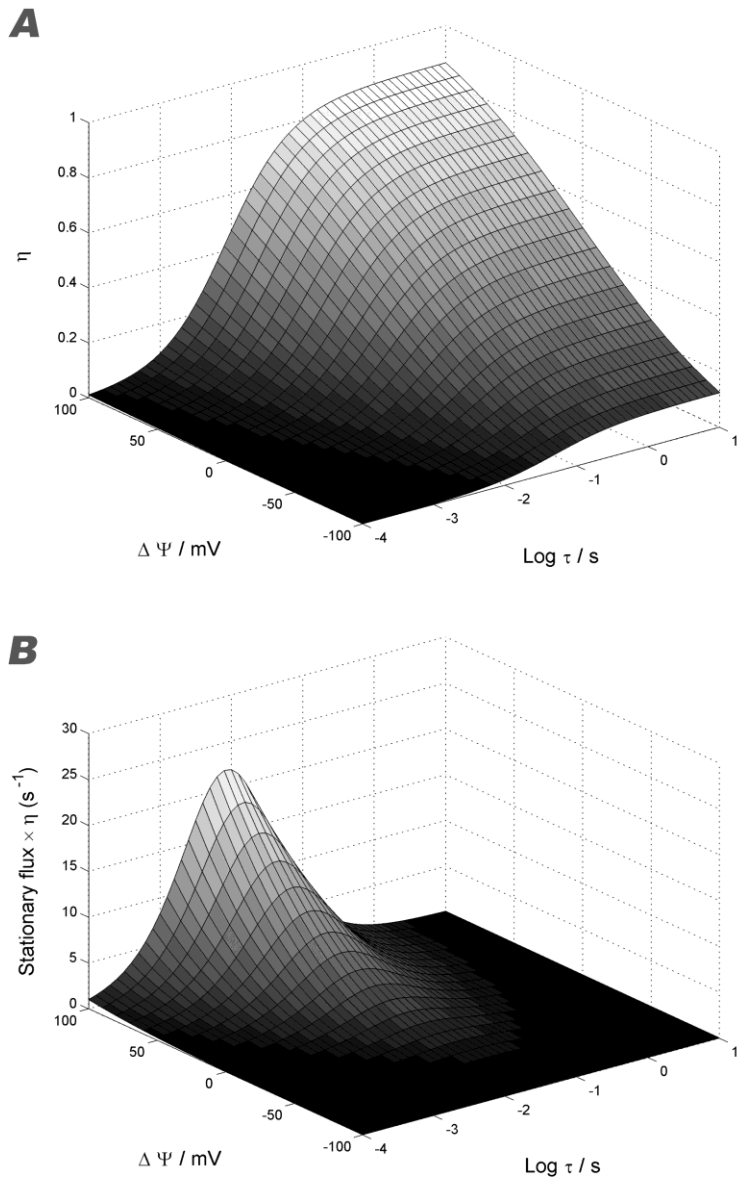

Fig. 4. (A) The coupling efficiency, η, of the single-ion model *vs.* membrane potential and the decimal logarithm of cycle duration, for electrical distances $d_{12} = 0;\quad d_{23} = d_{34} = 0.5;\ d_{41} = 0$ and $\mathrm{pH} = 7$ on both sides. (B) The product of the stationary ion flux per pump and η. Rate constants are given in the caption of Fig. 1.

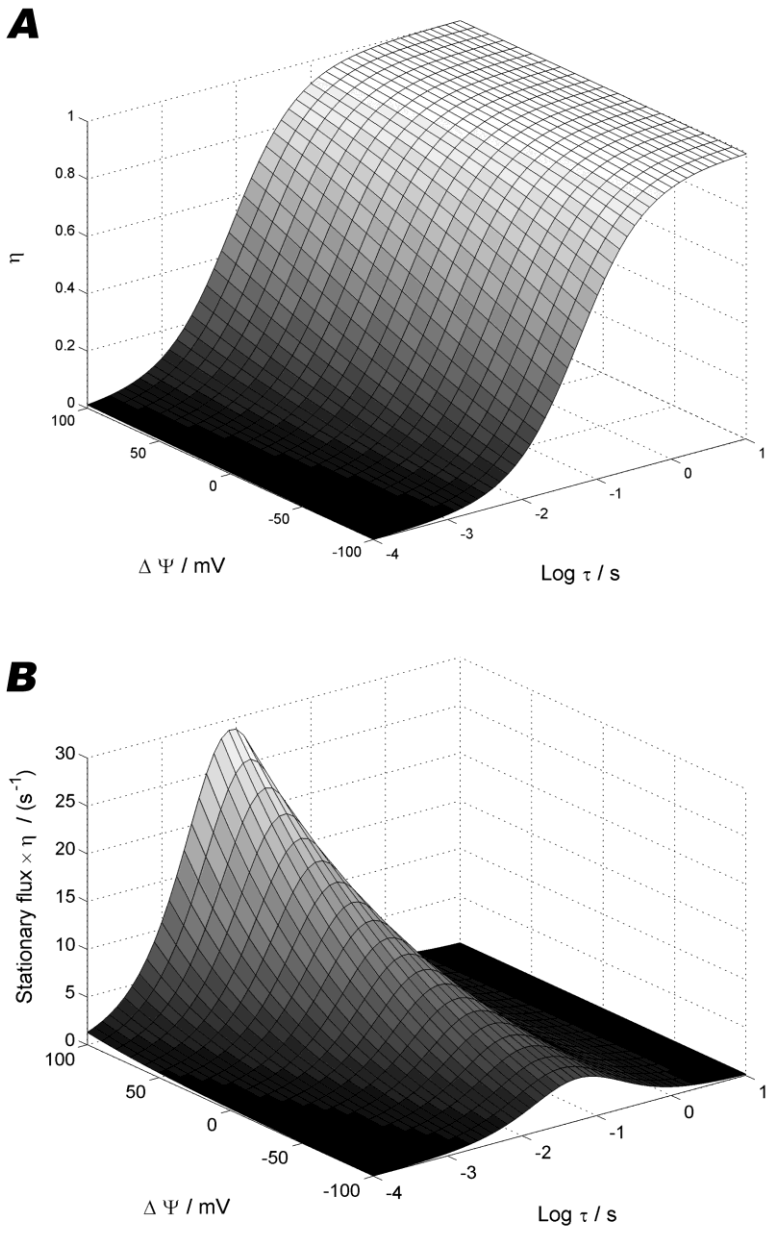

Fig. 5. (A) The coupling efficiency, η, of the multi-ion model *vs.* membrane potential and the decimal logarithm of the cycle duration. (B) The stationary flux of a pump multiplied by the coupling efficiency. Model parameters are the same as in Fig. 4.

DISCUSSION

Besides its simplicity, an advantage of the analytic approach proposed here resides in its ability to investigate model predictions over a wide range of parameters. Using numerical methods, such an investigation would require numerous compute-intensive simulations.

The stationary flux displays a bell-shaped pH-dependency for the multi-ion model (see Fig. 3, circular markers). This feature of the multi-ion model qualitatively agrees with experimental data on bacteriorhodopsin [16, 18]. The single-ion model proves unsatisfactory from this point of view. Indeed, bacteriorhodopsin, a light-driven proton pump from the membrane of the archaebacteria *Halobacterium salinarum* incorporates at least three proton-binding sites, two of them being occupied during most of the pumping cycle [11, 12]. Nevertheless, a rigorous validation of the SERC model would require quantitative comparisons with experimental data on proton pumping by bacterial rhodopsins. For example, absorption kinetic and electric measurements [16] could be performed during rapid changes in pH via the photorelease of caged protons [1].

In the single-ion version of the SERC model, the coupling efficiency, η, exceeds 50% only for positive membrane potentials, when outward proton flux is electrically favored (Fig. 4A). The flipping rate also plays an important role, comparable to the membrane potential.

Figures 4 and 5 allow to identify ranges of the membrane potential and flipping rate for which both good coupling ratio and high flux are achieved. Fig. 4B indicates no such parameter domain for the single-ion model at negative membrane voltages.

Our analytic results are in accord with Monte Carlo simulations [19], which have also shown that, under certain conditions, the coupling efficiency of the multi-ion model approaches unity. Figure 5A reveals a wide range of parameters for which $\eta \to 1$, whereas Fig. 5B shows that the multi-ion system is capable of efficient pumping at physiological membrane potentials (–50 mV to –100 mV for most cell types).

The SERC model is conceptually related to a recently proposed model of a stochastically driven quantum dot, an electronic nano-device [2]. The model consists of a single-level quantum dot subject to a stochastic external force that causes the energy of the dot to switch between two values. As a result, the dot works as a current rectifier, causing electrons to flow against the chemical bias. Just as in the case of the SERC model of active transport, the stochastically driven

quantum dot converts one type of work (the one involved in switching the dot energy) into another (the pumping of electrons against the electrochemical potential gradient) [2].

CONCLUSION

The qualitative agreement with experiments suggests that, in spite of its simplicity, the present theory incorporates some essential features of the mechanism of vectorial ion transport. Besides improving the conceptual framework of the SERC model, the formalism described here allows for the study of model predictions without time-consuming computer simulations. For instance, it proved to be an efficient tool for investigating the pumping rate and coupling efficiency (Figs. 4 and 5).

We believe the mathematical technique employed in the present work may be applied to a large variety of kinetic models that incorporate changes of free energy profiles occurring at random instants of time.

Acknowledgements. I thank Eiro Muneyuki for exciting discussions and for the critical reading of this article.

REFERENCES

1. ELLIS-DAVIES, G.C.R., Caged compounds: photorelease technology for control of cellular chemistry and physiology, *Nature Methods*, 2007, **4**, 619–628.
2. ESPOSITO, M., N. KUMAR, K. LINDENBERG, C. VAN DEN BROECK, Stochastically driven single-level quantum dot: A nanoscale finite-time thermodynamic machine and its various operational modes, *Physical Review E*., 2012, **85**, 031117.
3. FULINSKI, A., Active transport in biological membranes and stochastic resonances, *Phys. Rev. Lett.*, 1997, **79**, 4926.
4. FULINSKI, A., Barrier fluctuations and stochastic resonance in membrane transport, *Chaos*, 1998, **8**, 549–556.
5. GADSBY, D.C., R.F. RAKOWSKI, P. DE WEER, Extracellular access to the Na,K pump: pathway similar to ion channel, *Science*, 1993, **260**, 100–103.
6. HAMMES, G.G., Unifying concept for the coupling between ion pumping and ATP hydrolysis or synthesis, *Proc. Natl. Acad. Sci. USA*, 1982, **79**, 6881–6884.
7. HILL, T.L., *Free Energy Transduction in Biology*, Academic Press, New York, 1977.
8. HILLE, B., Ionic selectivity, saturation, and block in sodium channels. A four-barrier model. *J. Gen. Physiol.*, 1975, **66**, 535–560.
9. HILLE, B., *Ionic Channels of Excitable Membranes*, Sinauer Associates, Sunderland, MA, 1992.
10. HORSTHEMKE, W., R. LEFEVER, *Noise-Induced Transitions*, Springer Verlag, Berlin, 1984.
11. LANYI, J.K., Bacteriorhodopsin as a model for proton pumps, *Nature*, 1995, **375**, 461–463.

12. LANYI, J.K., Crystallographic studies of the conformational changes that drive directional transmembrane ion movement in bacteriorhodopsin, *Biochim. Biophys. Acta*, 2000, **1459**, 339–345.
13. LÄUGER, P., A channel mechanism for electrogenic ion pumps, *Biochim. Biophys. Acta*, 1979, **552**, 143–161.
14. LÄUGER, P., *Electrogenic Ion Pumps*, Sinauer Associates, Sunderland, MA, 1991.
15. LOGINOV, V.M., Simple mathematical tool for statistical description of dynamical systems under random actions, *Acta Physica Polonica B*, 1996, **27**, 693–735.
16. LUDMANN, K., C. GERGELY, A. DÉR, G. VÁRÓ, Electric signals during the bacteriorhodopsin photocycle, determined over a wide pH range, *Biophys. J.*, 1998, **75**, 3120–3126.
17. LUECKE, H., B. SCHOBERT, H.T. RICHTER, J.P. CARTAILLER, J.K. LANYI, Structural changes in bacteriorhodopsin during ion transport at 2 angstrom resolution, *Science*, 1999, **286**, 255–261.
18. MUNEYUKI, E., M. IKEMATSU, M. YOSHIDA, $\Delta\mu H^+$ dependency of proton translocation by bacteriorhodopsin and a stochastic energization-relaxation channel model., *J. Phys. Chem.*, 1996, **100**, 19687– 19691.
19. MUNEYUKI, E., T.A. FUKAMI, Properties of the stochastic energization-relaxation channel model for vectorial ion transport, *Biophys. J.*, 2000, **78**, 1166–1175.
20. MUNEYUKI, E., K. SEKIMOTO, Allosteric model of an ion pump, *Phys. Rev. E*, 2010, **81**, 011137.
21. SHAPIRO, V.E., V.M. LOGINOV, "Formulae of differentiation" and their use for solving stochastic equations, *Physica A***,** 1978, **91**, 563– 574.
22. TANFORD, C., Mechanism of free energy coupling in active transport, *Annu. Rev. Biochem.*, 1983, **52**, 379–409.
23. VAN DEN BROECK, C., On the relation between white shot noise, Gaussian white noise and the dichotomic Markov process, *J. Stat. Phys.*, 1983, **31**, 467–483.